中国科技论文在线 www.paper.edu.cn

International Journal of Fracture **98:** 151–177, 1999.
© 1999 *Kluwer Academic Publishers. Printed in the Netherlands.*

Determination of double-*K* criterion for crack propagation in quasi-brittle fracture, Part II: Analytical evaluating and practical measuring methods for three-point bending notched beams

SHILANG XU and H.W. REINHARDT
Institute of Construction Materials, University of Stuttgart, Pfaffenwaldring 4, 70550 Stuttgart, Germany
e-mail: reinhardt@iwb.uni.stuttgart.de

Received 21 November 1997; accepted in revised form 20 May 1999

Abstract. In this paper, an attempt is made to determine the double-K fracture parameters K_{Ic}^{ini} and K_{Ic}^{un} using three-point bending notched beams. First, based on the knowledge from extensive investigations which showed that the nonlinearity of P-CMOD curve is mainly associated with crack propagation, a linear asymptotic superposition assumption is proposed. Then, the critical effective crack length a_c is analytically evaluated by inserting the secant compliance c_s into the formula of LEFM. Furthermore, an analytical result of a fictitious crack with cohesive force in an infinite strip model was obtained. The double-K fracture parameters K_{Ic}^{ini} and K_{Ic}^{un} as well the critical crack tip opening displacement CTOD_c were analytically determined. The experimental evidence showed that the double-K fracture parameters K_{Ic}^{ini} and K_{Ic}^{un} are size-independent and can be considered as the fracture parameters to describe cracking initiation and unstable fracture in concrete structures. The testing method required to determine K_{Ic}^{ini} and K_{Ic}^{un} is quite simple, without unloading and reloading procedures. So, for performing this test, a closed-loop testing system is not necessary.

Key words: Double-K criterion, asymptotic superposition of assumption, three-point bending beams, double-K fracture parameters, fracture mechanics, concrete.

1. Introduction

Three-point bending notched beams are often used to measure the fracture parameters of concrete materials. The double-K fracture parameters (K_{Ic}^{ini} and K_{Ic}^{un}) introduced in (Shilang and Reinhardt, 1997) can be determined by the three-point bending notched beams too.

In principle, the definition of K_{Ic}^{un} used in the double-K fracture criterion (Shilang and Reinhardt, 1997) is similar to that of K_{Ic}^{s} used in the two parameter fracture model by Jenq and Shah (1985a; 1985b) and K_{Ic}^{e} used in the effective crack model by Karihaloo and Nallathambi (1986; 1989; 1990) and Swartz and Go (1984) as well as by Swartz and Refai (1987a; 1987b). In the determination for K_{Ic}^{s} and K_{Ic}^{e}, an equivalent-elastic crack concept were introduced. However, the methods for evaluating the length of the effective crack proposed by the various research groups (Jenq and Shah, 1985a; 1985b; Nallathambi and Karihaloo, 1986; 1989; 1990; Swartz and Go, 1984; Swartz and Refai, 1987a; 1987b; Tang et al., 1985; Bazant and Kazemi, 1990) are significantly different.

In the work of Swartz's research group (Swartz and Go, 1984; Swartz and Refai, 1987a; 1987b), as a primary method, Swartz and Go (1984) proposed to use the value of CMOD[1] measured at point D (see Figure 1, where $P = 0.95P_{\max}$ after the maximum load) in a P-CMOD curve for determining the effective crack length, a_e.

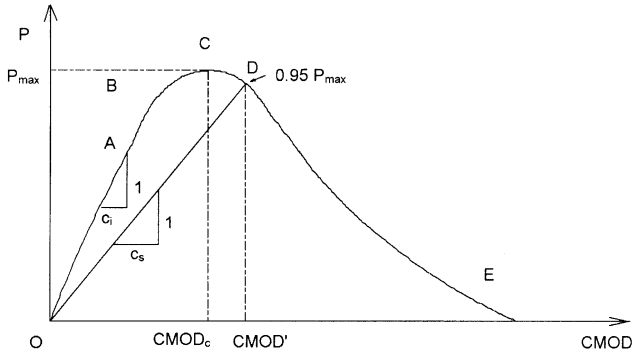


Figure 1. Determination method for critical effective crack length using CMOD′ measured at the point D($P = 0.95\ P_{\max}$ after maximum load) on P-CMOD curve by Swartz and Go (1984).

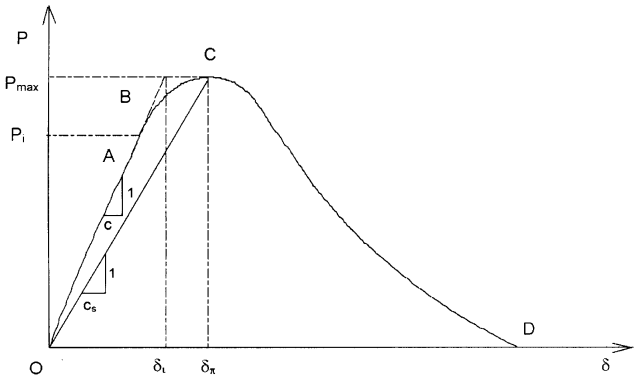


Figure 2. Determination method for critical effective crack length using the value of deflection δ_p measured at the peak load point B on the load-deflection curve by Karihallo and Nallathambi (1989; 1990; 1984).

Since the value of CMOD[1] measured at point D is larger than the value of CMOD_c measured at the maximum load point C, Swartz and Refai (1987a) said that this clearly led to an overestimation of compliance c_s and hence a_e. So, some regression curves based on experimental observation were introduced to determine a_e for notched beams (Swartz and Refai, 1987b). The experimental observations were carried out on a series of precracked beams using a dye-penetrant technique (Swartz and Refai, 1987a; 1987b). It turned out that for different geometries, even for beams with proportional dimensions, one needs always a regression analysis to obtain the corresponding a_e.

In the effective crack model proposed by Karihaloo and Nallathambi in (1986; 1989; 1990), the authors employed such an approach to insert the measured value of deflection δ_p, corresponding to the maximum load point C at the load-deflection P-δ curve, see Figure 2, into an integral equation to determine the effective crack length a_e. It is not so easy to get a closed form solution for this problem. Hence, they used a trial and error method to calculate a_e. Finally, they proposed a regression expression to calculate a_e too (Karihaloo and Nallathambi, 1990). However the valid application region of the regression expression is limited.

Since in the two parameter fracture model (TPFM) proposed by Jenq and Shah in (1985a; 1985b) the effective crack length a_e is evaluated by linear elastic fracture mechanics, only the elastic part CMOD_c^e of the total CMOD_c (see Figure 3) is taken into account. For measuring it, an unloading procedure has to be performed in the tests. In the calculation of the relative

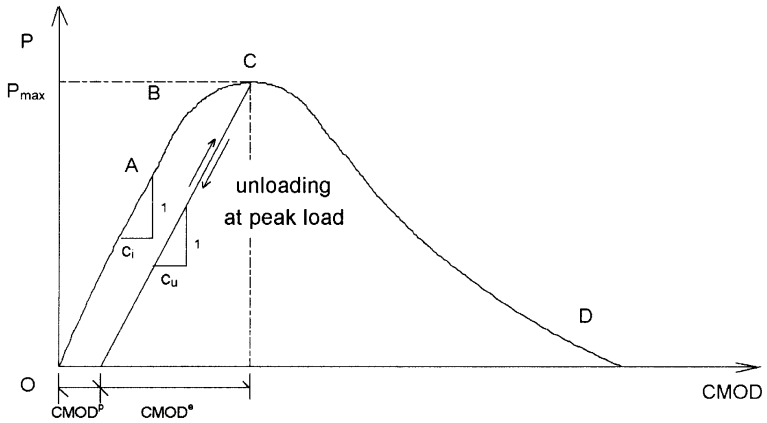


Figure 3. Determination method for the effective crack length using the elastic part $CMOD^e$ of the total $CMOD_c$ proposed by Jeng and Shah (1985a; 1985b).

parameters a_e, K_{Ic}^s and $CTOD_c$, the inelastic part $CMOD_c^P$ of the total $CMOD_c$ is ignored. In recent years, it has been widely recognized that the nonlinear fracture characteristic of concrete is mainly associated with the fracture process zone or stable crack propagation. Therefore, to ignore the inelastic part, $CMOD_c^P$, possibly led to an underestimate of the critical crack length a_c. Besides, it needs a closed-loop testing system for achieving stable unloading after the maximum load. However, some advantages in the two parameter fracture model are favorable. For example, only a single size of three-point bend beams is needed in the tests.

Recently, Tang, Ouyang and Shah have pointed out that the testing facilities with a close-loop system required for achieving stable unloading after the maximum load 'has been somehow restricted the application of TPFM' (Tang et al., 1995). For avoiding the restriction, they proposed a peak load method (Tang et al., 1995). This method needs to test several three-point bend beams or several splitting tension cylinders. So, a main advantage of the two parameter fracture model that is to use only a single size of specimens in the experiments vanished in the recently proposed peak load method.

In the determination method of the double-K fracture parameters, K_{Ic}^{ini} and K_{Ic}^{un}, it is also needed to evaluate the effective crack length a_e. Then, the analytical solution of the equivalent stress intensity factor K_I^c caused by the cohesive force on the fictitious crack is consequently solved. At the critical situation, the equivalent stress intensity factor is called cohesion toughness K_{Ic}^c. After the unstable fracture toughness K_{Ic}^{un} is evaluated, the initiation toughness K_{Ic}^{ini} can be obtained by using the relationship between double-K fracture parameters K_{Ic}^{ini} and K_{Ic}^{un} and the cohesion toughness K_{Ic}^c.

The unstable fracture toughness K_{Ic}^{un}, initiation toughness K_{Ic}^{ini} and the critical crack tip opening displacement $CTOD_c$ as well as the critical crack length a_c are analytically evaluated, without regression analysis. For determining them, tests on a single size of three-point bending notched beams are needed. In the testing procedure, unloading is not necessary. Even without a closed-loop testing system, it is possible to perform the tests.

2. A linear asymptotic superposition assumption

According to the extensive investigations by many researchers, the nonlinearity of the P-CMOD curve measured on concrete is mainly due to the slow crack extension (or stable

中国科技论文在线 www.paper.edu.cn

propagation) in front of the preformed crack. Therefore, the crack extension is taken into account to evaluate the fracture parameters introduced in some fracture models for concrete materials, like the two parameter fracture model (1985a; 1985b), the effective crack model (Nallathambi and Karihaloo, 1986; 1989; 1990; Swartz and Go, 1984; Swartz and Refai, 1987a; 1987b) and the size effect model (Bazant and Kazemi, 1990). In the fracture models, the effective crack is defined as an equivalent-elastic crack although the crack in the fracture process is certainly not only elastic. For employing the approaches of linear elastic fracture mechanics (LEFM) to describe the complete fracture process and to determine the double-K fracture parameters, a linear asymptotic superposition assumption is introduced. This assumption is only based on the following two hypotheses:

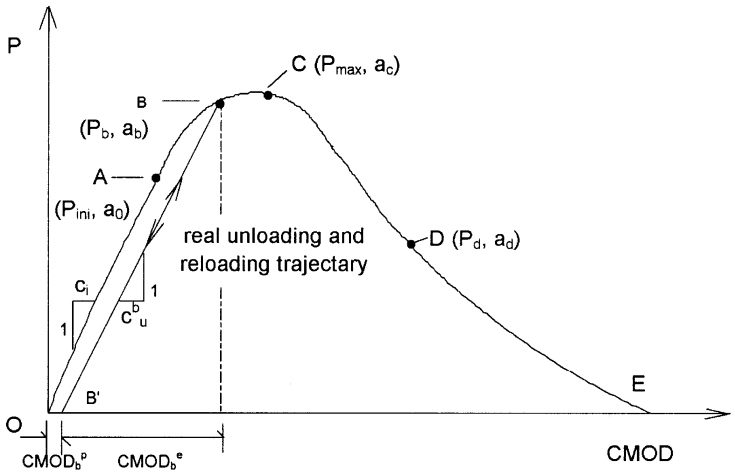
(1) the nonlinear characteristic of the P-CMOD curve is caused by fictitious crack extension in front of a stress-free crack;
(2) an effective crack consists of an equivalent-elastic stress-free crack and an equivalent-elastic fictitious crack extension.

Before introducing the linear asymptotic superposition method, let us investigate a loading-unloading-reloading procedure in a test that is carried out on a concrete three-point bending notched beam with a preformed notch a_0, see Figure 4(a). A practical example of loading-unloading-reloading cycles in terms of P-CMOD for a concrete bending beam can be found in the work of Hu and Wittmann (1991).

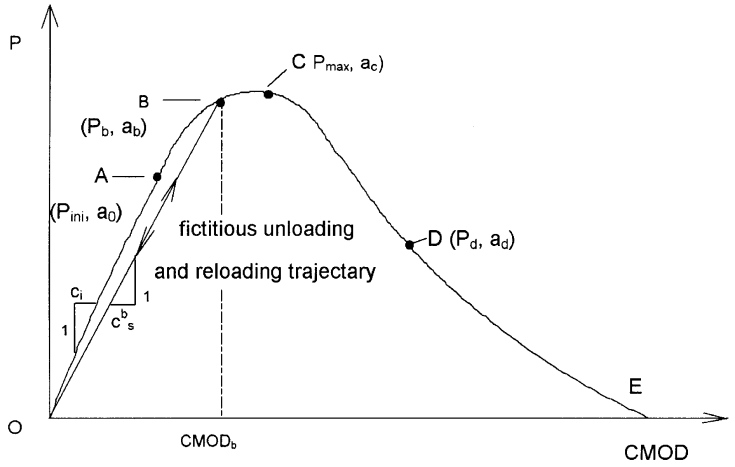
Between point O and point A, a preformed crack does not cause any slow extension. Hence, the P-CMOD curve is linear in this region. At point A, the preformed crack starts its slow extension and the P-CMOD curve begins to appear nonlinear. No doubt, in the region between point O and point A, the length of the preformed crack keeps constant a_0 and linear elastic fracture mechanics approaches can be directly employed to calculate the stress intensity factor at the preformed crack tip caused by an arbitrary external load. So, the initiation toughness K_{Ic}^{ini} can be obtained by inserting the external load P_{ini} and the length of preformed crack a_0 into a formula developed from linear elastic fracture mechanics. Once beyond point A, the approaches of LEFM are regarded as no longer available. Note, that the line OABCDE shown in Figure 4(a) should be a plot of P-CMOD in monotonous loading conditions for a three-point bending beam with crack length a_0.

Corresponding to point B, the effective crack length is denoted with a_b, where $\Delta a_b = a_b - a_0$ is an extension of cracking and can be termed as a fictitious crack extension, and the loading value at point B is P_b. Then, unloading is performed until the load value comes back to zero. Now, the beam can be regarded as one with an effective initial crack a_b which was precracked (of course, Δa_b is not stress-free and some cohesive force is acting on it). If reloading is carried out, the P-CMOD curve will develop along the line B′BCDE shown in Figure 4(a). Therefore, in the region between point B′ and point B, the length of the precracked crack keeps constant a_b and the approaches of LEFM are suitable too. Specially at point B, the stress intensity factor $K_{\mathrm{I}b}$ at the effective crack tip caused by the external load P_b can be evaluated by the approaches of LEFM.

However, care must be taken in the reasonable evaluation of the effective crack length a_b. If one just uses the elastic part CMOD_b^e or the compliance C_u^b measured on the reloading line B′ B to evaluate a_b, it may lead to an underestimate of a_b because the nonlinearity on the AB segment results from both the inelastic part CMOD_b^p of the total CMOD_b and the difference of elastic compliance between the initial elastic compliance c_i and the reloading elastic compliance c_u^b. Hence, the influence of the inelastic part, CMOD_b^p of the total CMOD_b



(a) Real unloading and reloading trajectary at an arbitrary load point.



(b) Fictitious unloading and reloading trajectory at an arbitrary load point.

Figure 4. Illustration of unloading and reloading trajectories: (a) a real situation; and (b) a fictitious situation.

on the crack extension should be taken into account according to hypothesis (1). Further considering the hypothesis (2), the progressively extending crack with somewhat inelastic characteristic should be equivalent to an elastic crack taking account of the influence of the inelastic part CMOD_b^p of the total CMOD_b on the crack propagation.

Now, we consider the case that an elastic progressively extending crack consists of an equivalent-elastic stress-free crack and an equivalent-elastic fictitious crack extension. If unloading starts at point B at which the equivalent-elastic crack has extended its length a_b the unloading trajectory will go down to the original point O along a fictitious trajectory OB, see Figure 4(b).

The unloading trajectory is termed the fictitious trajectory due to the assumption of zero permanent deformation after unloading.

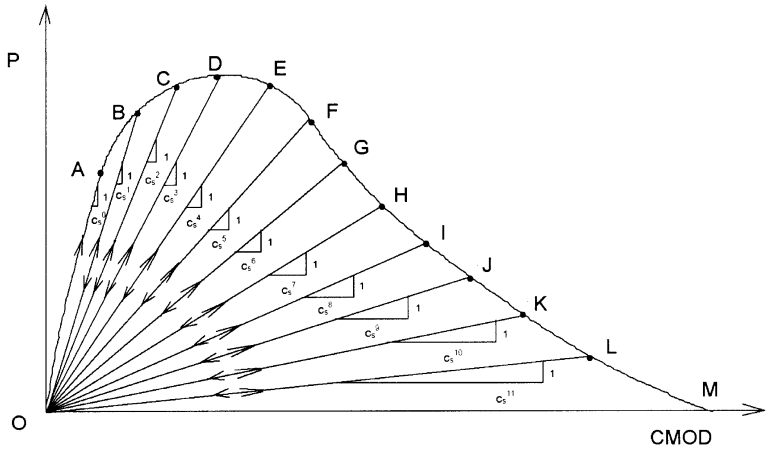


Figure 5. Illustration of asymptotical superposition of initially linear P-CMOD curves.

The reloading trajectory will rise up along the same unloading trajectory OB. Corresponding to the extension of the equivalent-elastic crack from a_0 to a_b, the compliance changes from c_i to c_s. Therefore, it could be expected that when a three-point bending beam denoted with A with a crack, of which an initially preformed length is a_0, is tested, the measured P-CMOD curve will be along the line OABCDE shown in Figure 4(b), and if one did a test on a beam denoted with B that has the same material and geometrical dimensions as the beam A, but an equivalent-elastic crack with length a_b instead of the initially preformed crack length a_0, the possibly measured P-CMOD curve should be along the line OBCDE shown in the Figure 4(b). So, the P-CMOD curve with the line OBCDE could be assumed to be measured from the beam B which should have been precracked to grow the equivalent-elastic crack to a desirable size a_b. Beyond point B, with increase of load, the crack will further develop and P-CMOD curves measured from both beams A and B are the same. The difference between the initial crack lengths a_0 and a_b in beam A and beam B only results in the difference between two trajectories OAB and OB for beams A and B until loading value P_b is achieved.

Now, we further assume that a series of beams which are made from the same material and have the same geometry and the same dimensions are precracked to grow the equivalent-elastic cracks to their different lengths $a_0, a_1, a_2, \ldots a_i$. Then a load is applied to each beam until nonlinear deformation appears on the measured P-CMOD curve. Hence, a series of P-CMOD curves OA, OB, OC, OD, OE, . . . , and so on, will be straight lines. These straight lines OA, OB, OC, OD, OE, . . . , are drawn in the same coordinate or are asymptotically superimposed together as the illustration in Figure 5. When the number of straight lines is big enough, from the original point O of the coordinate to all ends of the straight lines A, B, C, D, E, . . . , M, a smooth curve can be drawn. It can be expected that this envelope will coincide with the measured P-CMOD curve of a beam with an initial crack a_0. The beams are made of the same material and dimensions used in the series of beams. This assumption is called linear asymptotic superposition assumption.

After onset of slow crack extension or appearance of nonlinear deformation, from an arbitrary point B on a complete P-CMOD curve to its original point O, one can draw a secant line OB. According to the linear asymptotic superposition, the secant line OB can be regarded as the linear segment of a P-CMOD curve measured from a beam with a corresponding equivalent-elastic crack length a_b. At the end point of the linear segment of any P-CMOD

中国科技论文在线 www.paper.edu.cn

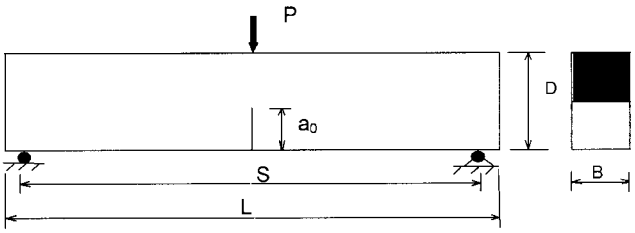


Figure 6. Configuration of three-point bending notched beam.

curve, linear elastic fracture mechanics is suitable. Thus, a complete fracture process with nonlinear fracture characteristics can be solved through asymptotically superimposing a series of linear solutions obtained by the approaches of LEFM. In other words, a solution of one point on a nonlinear P-CMOD curve can be equivalently solved by the approaches of LEFM because any point on the nonlinear P-CMOD curve can be treated as a special case of the assembly of a series of linear cases.

3. Evaluation of the effective crack length

After a three-point bending notched beam of concrete is tested, of which the configuration is illustrated in Figure 6, the typical P-CMOD curve is shown in Figure 7.

According to the above-mentioned linear asymptotic superposition assumption the equivalent-elastic crack length at maximum load can be solved by LEFM as follows (Tada et al., 1985):

$$\text{CMOD} = \frac{6PSa}{D^2BE}V_{\text{I}}(\alpha) \tag{1}$$

for $S/D = 4$, the function $V_{\text{I}}(\alpha)$ is given as follows:

$$V_{\text{I}}(\alpha) = 0.76 - 2.28\alpha + 3.87\alpha^2 - 2.04\alpha^3 + \frac{0.66}{(1-\alpha)^2}, \tag{2}$$

where α = $(a + H_0)/(D + H_0)$;
P = the maximum load;
S = specimen loading span;
D = beam depth;
B = beam width;
H_0 = thickness of clip gauge holder.

Young's modulus E can be calculated from the measured initial compliance c_i through a method proposed by RILEM (1990) as follows:

$$E = \frac{6Sa_0V_{\text{I}}(\alpha_0)}{C_iBD^2} = \frac{24}{C_iB}\frac{a_0}{D}V_{\text{I}}(\alpha_0) \tag{3}$$

where α_0 = $(a_0 + H_0)/(D + H_0)$
a_0 = initial crack length.

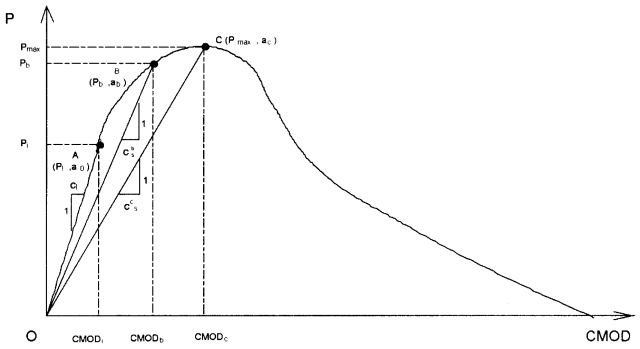


Figure 7. Determination method of effective crack length for an arbitrary loading point using the secant compliance c_s according to the linear asymptotic superposition assumption proposed.

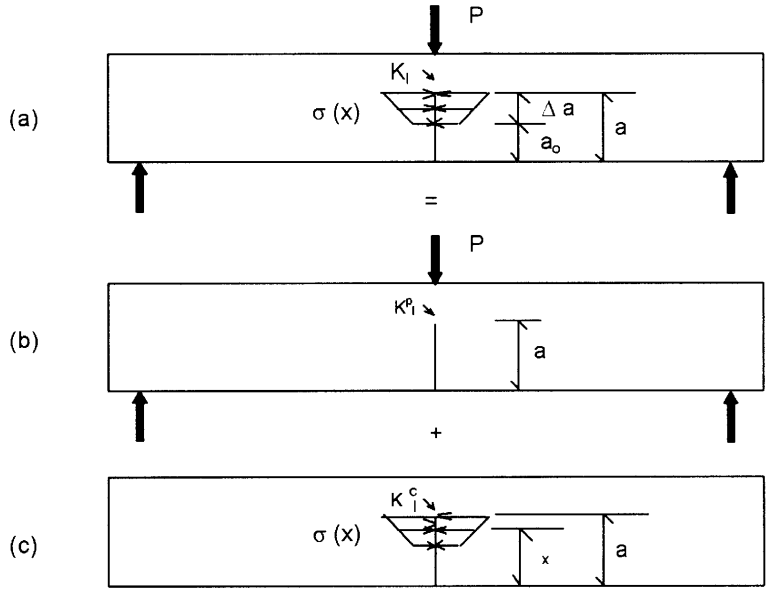


Figure 8. Superposition method for calculating K_{I}.

Karihaloo and Nallathambi's tests (1991) showed that the average values of Young's modulus E measured from P-CMOD curves, P-δ curves and the compressive cylinder tests are almost the same. So, if the P-CMOD curves are not measured in some cases, Young's modulus E that is measured from the standard compressive cylinder tests can be used to predict the average of the critical crack length of a group of specimens.

4. Analytical approaches to calculate K_{I}^{c} in the case of a finite crack with a fictitious crack zone in an infinite strip

In this section, it is necessary to use the analytical approach proposed in (Jenq and Shah, 1985a) to calculate K_{I}^{c} created by the cohesive force at the tip of a fictitious crack in an infinite strip.

A superposition scheme for calculating the stress intensity factor at the effective crack tip in a three-point bending notched beam caused by the external load P and the cohesive force on

中国科技论文在线 www.paper.edu.cn

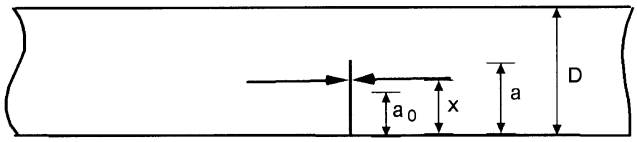


Figure 9. Infinite strip subjected to a unit point load.

the fictitious crack zone can be illustrated in Figure 8. The stress intensity factor K_{I}^{p} caused by the external load P shown in Figure 8(b) can be directly calculated by the formula of LEFM. So, we only need to discuss the evaluation of K_{I}^{c} caused by the cohesive force on the fictitious crack zone shown in Figure 8(c) in details herein.

An infinite strip subjected to a unit point load is demonstrated in Figure 9. The K_{I} value of a crack in the infinite strip of unit thickness subjected to a pair of unit point load can be expressed as

$$K_{\mathrm{I}} = \frac{2}{\sqrt{\pi a}} F\left(\frac{x}{a}, \frac{a}{D}\right), \tag{4}$$

where

$$F\left(\frac{x}{a}, \frac{a}{D}\right) = \frac{3.52\left(1-\frac{x}{a}\right)}{\left(1-\frac{a}{D}\right)^{3/2}} - \frac{4.35 - 5.28\frac{x}{a}}{\left(1-\frac{a}{D}\right)^{1/2}} + \left\{\frac{1.30 - 0.30\left(\frac{x}{a}\right)^{3/2}}{\left[1-\left(\frac{x}{a}\right)^{2}\right]^{1/2}} + 0.83 - 1.76\frac{x}{a}\right\}\left\{1 - \left(1-\frac{x}{a}\right)\frac{a}{D}\right\}.$$

For a critical situation at which the maximum external load is achieved and the crack tip opening displacement arrives at its critical value CTOD_c, the corresponding cohesive force distribution on the fictitious crack zone shown in Figure 10 can be expressed as

$$\sigma(x) = \sigma_s(\mathrm{CTOD}_c) + \frac{x - a_0}{a - a_0}[f_t - \sigma_s(\mathrm{CTOD}_c)]$$

or

$$\sigma\left(\frac{x}{a}\right) = \sigma_s(\mathrm{CTOD}_c) + \frac{\frac{x}{a} - \frac{a_0}{a}}{1 - \frac{a_0}{a}}[f_t - \sigma_s(\mathrm{CTOD}_c)]$$

$$0 \leqslant \mathrm{CTOD} \leqslant \mathrm{CTOD}_c, \quad \text{or } a_0 \leqslant x \leqslant a_c. \tag{5}$$

The σ_s in Equation (5) is the value of the cohesive force at the preformed crack tip when CTOD arrives at its critical value CTOD_c. It can be determined by an expression proposed by Reinhardt et al. (1986) as follows:

$$\frac{\sigma}{f_t} = \left\{1 + \left(c_1\frac{w}{w_0}\right)^3\right\}\exp\left(-c_2\frac{w}{w_0}\right) - \frac{w}{w_0}(1 + c_1^3)\exp(-c_2), \tag{6}$$

where the coefficient c_1, c_2 are material constants and w_0 is the maximum crack opening width when the stress became zero. Those values are measured in (Reinhardt et al., 1986). In Equation (6), w is replaced by the measured CTOD_c value. Then σ_s can be obtained.

中国科技论文在线 www.paper.edu.cn

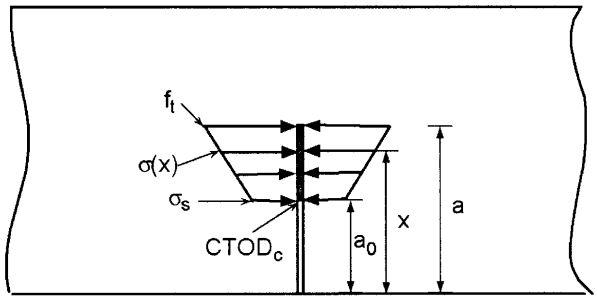


Figure 10. The cohesive force distribution on the fictitious crack zone at a critical situation.

The σ-w relation can be simplified to a bilinear softening one as follows:

$$\begin{aligned} \sigma &= f_t - (f_t - \sigma_s)\frac{w}{w_s}, \quad 0 \leqslant w \leqslant w_s \\ \sigma &= \sigma_s \frac{w_0 - w}{w_0 - w_s}, \quad w_s \leqslant w \leqslant w_0 \\ \sigma &= 0, \quad w \geqslant w_0. \end{aligned} \tag{7}$$

According to our investigation, $w_s = \mathrm{CTOD}_c$. Using the approaches proposed by CEB-FIP Model Code 1990 (1993), a modified method is presented to determine the parameter β as follows:

$$\beta = \sigma_s / f_t = \frac{1}{\alpha_F}(2 - f_t\ \mathrm{CTOD}_c / G_F), \tag{8}$$

where, $\alpha_F = 9 - d_{\max}/8$ and $w_0 = \alpha_F G_F / f_t$. G_F can be determined according to the approaches of CEB-FIP Model Code 1990 (1993) too. $d_{\max}$ is the maximum size of coarse aggregate of concrete.

Now, the overall K_{I}^c value due to the cohesive force distributed on the fictitious crack zone at the critical situation can be calculated by using expression (4) as a Green's function as follows:

$$K_{\mathrm{I}}^c = -\int_{a_0}^{a_c} \frac{2\sigma\left(\frac{x}{a_c}\right)}{\sqrt{\pi a_c}} F\left(\frac{x}{a_c}, \frac{a_c}{D}\right) \mathrm{d}x \tag{9}$$

let

$$\frac{a_c}{D} = V, \quad \frac{x}{a_c} = U, \quad \mathrm{d}x = a_c\, \mathrm{d}U,$$

then, when $x = a_c,\ U = 1;\ x = a_0,\ U = a_0/a_c$, so, Equation (9) can be rewritten as

$$K_{\mathrm{I}}^c = -\int_{a_0/a_c}^{1} 2\sqrt{\frac{a_c}{\pi}}\sigma(U) F(U, V)\, \mathrm{d}U \tag{10}$$

correspondingly, where

$$\begin{aligned} F(U, V) &= \frac{3.52(1-U)}{(1-V)^{3/2}} - \frac{4.35 - 5.28U}{(1-V)^{1/2}} \\ &\quad + \left\{ \frac{1.30 - 0.30U^{3/2}}{(1-U^2)^{1/2}} + 0.83 - 1.76U \right\} \cdot \{1 - (1-U)V\}. \end{aligned}$$

After the crack length is evaluated by (1) only U in (10) is variable. At the integral boundary of (10), the integration has a singularity. It is possible to gain the numerical results of the integration by using Gauss Chebyshev guadrature.

In respect to the fracture toughness of a material, the absolute value of the stress intensity factor K_{I}^{c} due to the cohesive force on the fictitious crack zone at the critical state can be regarded as a contribution to the total fracture toughness during the crack propagating. This part of the fracture toughness due to the cohesive force is called cohesion toughness termed with $K_{\mathrm{I}c}^{c}$. Therefore, for the considered problem the cohesion toughness $K_{\mathrm{I}c}^{c}$ can be evaluated as following expressions:

$$\begin{aligned} K_{\mathrm{I}c}^{c} &= |K_{\mathrm{I}}^{c}[\sigma_s, a_c]| \\ &= \int_{a_0}^{a_c} 2\sigma\left(\frac{x}{a_c}\right)\frac{1}{\sqrt{\pi a_c}}F\left(\frac{x}{a_c}, \frac{a_c}{D}\right)\mathrm{d}x \\ &= \int_{a_0/a_c}^{1} 2\sqrt{\frac{a_c}{\pi}}\sigma(U)F(U,V)\,\mathrm{d}U. \end{aligned} \tag{11}$$

As examples of numerical calculations for equation (11) the experimental data reported in Table 2 in (Jenq and Shah, 1985a) are utilized to calculate the values of $K_{\mathrm{I}c}^{c}$ at the critical situation. Specially, the values of effective crack length that were reported in Table 2 in (Jenq and Shah, 1985a) are used too due to lack of the measured CMOD_c^t in the table. Otherwise, (1) should have been used to calculate the corresponding values of the effective crack length. By the way, $K_{\mathrm{I}c}^{c}$ values calculated from the various specimens are presented in the column (5) in Table 1 in this paper based on the expression of softening traction-separation law expressed in (6) proposed by Reinhardt et al. (1986). CEB-FIP Model code 1990 (1993) proposed the approaches to determine the maximum crack opening width w_0 at the stress to be zero and the fracture energy G_F using the maximum size of coarse aggregate $d_{\max}$ and compressive strength f_c. According to the approaches, $w_0 = 160\ \mu$m and $G_F = 60.2$ N/m can be got. Then a trial and error method is used to gain $c_1 = 3,\ c_2 = 8.25$ for (6). It can be seen that $K_{\mathrm{I}c}^{c}$ values of the various specimens are not too small and cannot be neglected.

For the Griffith crack problem, the cohesion toughness $K_{\mathrm{I}c}^{c}$ had been gained by authors as following expression:

$$\begin{aligned} K_{\mathrm{I}c}^{c} &= \frac{2}{1-\frac{a_0}{a_c}}\sqrt{\frac{a_c}{\pi}}\left\{\left[\sigma_s(\mathrm{CTOD}_c) - \frac{a_0}{a_c}f_t\right]\mathrm{arc\ cos}\,\frac{a_0}{a_c}\right. \\ &\quad \left. +[f_t - \sigma_s(\mathrm{CTOD}_s)]\sqrt{1-\left(\frac{a_0}{a_c}\right)^2}\right\}. \end{aligned} \tag{12}$$

And for the semi-infinite crack problem, the corresponding $K_{\mathrm{I}c}^{c}$ is expressed in a very simple form:

$$K_{\mathrm{I}c}^{c} = \frac{2}{3}\sqrt{\frac{2}{\pi}}[2f_t + \sigma_s(\mathrm{CTOD}_c)]\sqrt{\Delta a_c}. \tag{13}$$

Generally, both formulae (12) and (13) cannot be applied to the finite strip problem. But, if the minimum size conditions to measure the double-K fracture parameters can be met, the

.

Table 1. The K_{Ic}^{c} values evaluated by using Jeng and Shah's testing data (1985a).

Specimen	a_0/D	a_c/D	D (mm)	K_{Ic}^{c}(MPa m$^{1/2}$) using σ-ω relation (6) in (Reinhardt et al., 1986)			K_{Ic}^{c}(MPa m$^{1/2}$) using σ-ω relation (14) in (Gopalaratnam and Shah, 1985)		
				By Equation (11)	By Equation (12)	By Equation (13)	By Equation (11)	By Equation (12)	By Equation (13)
(1)	(2)	(3)	(4)	(5)	(6)	(7)	(8)	(9)	(10)
C1L1	0.333	0.347	229	0.205	0.202	0.202	0.200	0.198	0.197
C1L2	0.333	0.385	229	0.400	0.372	0.368	0.387	0.361	0.357
C1M1	0.318	0.377	152	0.366	0.336	0.332	0.356	0.328	0.324
C1M2	0.324	0.511	152	0.709	0.524	0.511	0.664	0.500	0.489
C1S1	0.293	0.498	76	0.573	0.407	0.395	0.540	0.390	0.380
C1S2	0.293	0.548	76	0.741	0.461	0.446	0.697	0.443	0.429
C1S3	0.293	0.535	76	0.682	0.443	0.429	0.641	0.425	0.412
C1S4	0.293	0.531	76	0.648	0.429	0.416	0.605	0.411	0.399

formulae can be used to estimate approximately. As known, when the length of stress-free crack is larger than ten times the length of the fictitious crack zone, the crack problem can be treated as a semi-infinite crack.

Only for the purpose of comparison, the formulae (12) and (13) were utilized to estimate the values of $K_{\mathrm{I}c}^{c}$ of the beams. The softening traction-separation law by (6) is used to determine the value of σ_s in formulae (12) and (13). The corresponding $K_{\mathrm{I}c}^{c}$ values estimated by formulae (12) and (13) are presented in the columns (6) and (7) in Table 1 respectively. Comparing the values of $K_{\mathrm{I}c}^{c}$ presented in the columns (5), (6) and (7) separately, it can be seen that when $\Delta a_c/a_0 = 5$ percent, the error between the values of $K_{\mathrm{I}c}^{c}$ obtained by formulae (11), (12) and (13) is 1.5 percent; and when $\Delta a_c/a_0 \leqslant 20$ percent, the errors is less than 10 percent that can approximately meet the accuracy requirement in engineering practice. It can also be found that when $\Delta a_c/a_0 \geqslant 50$ percent, the values of $K_{\mathrm{I}c}^{c}$ calculated by formula (11) are significantly larger than those calculated by both formulae (12) and (13), but, differences between the values of $K_{\mathrm{I}c}^{c}$ calculated by formulae (12) and (13) can be neglected.

In order to investigate the influence of the shape of the softening traction-separation law on $K_{\mathrm{I}c}^{c}$, the values of $K_{\mathrm{I}c}^{c}$ are recalculated by formulae (11), (12) and (13) based on the expression proposed by Gopalaratnam and Shah expressed in the following Equation (14) (Gopalaratnam and Shah, 1985), instead of Equation (6)

$$\frac{\sigma}{f_t} = \mathrm{e}^{-kw\lambda}, \tag{14}$$

where $\lambda = 1.01$ and $k = 0.06163$ for w in μm proposed for normal strength concrete in (Gopalaratnam and Shah, 1985). However, the parameters λ and k should be different when the measured values of fracture energy of concrete materials are different. For the concrete material used in the tests (Jenq and Shah, 1985a) the corresponding values of λ and k were determined to be 1.01 and 0.04 respectively according to the value of fracture energy of 60.2 N/m evaluated by the approaches of CEB-FIP Model Code 1990 (1993). The corresponding $K_{\mathrm{I}c}^{c}$ values calculated by formulae (11), (12) and (13) based on the relationship (14) are presented in the columns (8), (9) and (10) separately. It can be seen that there exists the influence of the shapes of softening traction-separation law on the values of $K_{\mathrm{I}c}^{c}$, but not too significant. It was also checked that the maximum error between the values of $K_{\mathrm{I}c}^{c}$ obtained by the parameters of $\lambda = 1.01$ and $k = 0.06163$ and those by the parameters of $\lambda = 1.01$ and $k = 0.04$ is less than 10 percent. So, in a general case for normal strength concrete, the constant parameters of $\lambda = 1.01$ and $k = 0.06163$ can be used.

5. Determination of double-K fracture parameters $K_{\mathrm{I}c}^{ini}$ and $K_{\mathrm{I}c}^{un}$

Now, our attention is focused on how to determine the double-K fracture parameters $K_{\mathrm{I}c}^{ini}$ and $K_{\mathrm{I}c}^{un}$ using three-point bending notched beams. As previously mentioned, $K_{\mathrm{I}c}^{un}$, is defined as the critical stress intensity factor created by the maximum load $P_{\max}$ at the effective crack tip. Therefore, for the three-point bending notched beam, the value of $K_{\mathrm{I}c}^{un}$ can be evaluated by inserting the maximum load $P_{\max}$ and critical crack length a_c into the following expression (Tada et al., 1985):

$$K_{\mathrm{I}} = \frac{3PS}{2D^2B}\sqrt{a}F_{\mathrm{I}}\left(\frac{a}{D}\right), \tag{15}$$

中国科技论文在线 www.paper.edu.cn

where the geometry factor $F_{\mathrm{I}}(a/D)$ depends on the ratio of span to depth of the beam and for S = 4D is given as follows (Tada et al., 1985)

$$F_{\mathrm{I}}\left(\frac{a}{D}\right)=\frac{1.99-\left(\frac{a}{D}\right)\left(1-\frac{a}{D}\right)\left[2.15-3.93\frac{a}{D}+2.7\left(\frac{a}{D}\right)^{2}\right]}{\left(1+2\frac{a}{D}\right)\left(1-\frac{a}{D}\right)^{3/2}}. \tag{16}$$

And the definition of the initiation toughness K_{Ic}^{ini} is given as the initial cracking stress intensity factor created by the initial cracking load P_{ini} at the initial crack tip. Because the initial crack length a_0 is a known value, it could be expected that if one knows the initial cracking load P_{ini}, the value of K_{Ic}^{ini} could be evaluated by using Equation (15) too.

For distinguishing the initial cracking load P_{ini} an investigator may employ two ways. One way is the direct measurement. As reported (Xu and Reinhardt, 1997), the experimental techniques, like the laser speckle interferometry, photoelastic coating, strain gauge technique and the acoustic emission method, should be utilized to distinguish the cracking initiation in the fracture tests. However, it is not convenient to use these experimental techniques in ordinary tests. Otherwise, these techniques only can be used to measure the surface crack that may differ from the interior of the specimen. Another way to distinguish the initial cracking load P_{ini} is to use the measured P-CMOD curve. One may take the starting point A of nonlinearity on the measured P-CMOD curve as the initial cracking point, see Figure 7. In practice, it is not so easy to detect the same point in the determination of the initial cracking point on a given P-CMOD curve from various investigators. Hence, an analytical approach for determining K_{Ic}^{ini} for the tests on three-point bending notched beams is proposed that is based on the analytical results of K_{Ic}^{c} herein.

At the beginning of crack propagation, the initial crack length is a_0 and the initial cracking load is P_{ini}, see Figure 7. At the situation, the initiation toughness is K_{Ic}^{ini} that represents ability of the body to resist an external load before the appearance of crack propagation in a structure. At the critical state, the fictitious crack zone in front of the initial stress-free crack has slowly extended. The critical crack length is a_c and the critical fracture load is the maximum load $P_{\max}$. The corresponding unstable fracture toughness is denoted with K_{Ic}^{un} that represents ability of the body to resist a maximum external load at the critical fracture situation. The difference between the initiation toughness K_{Ic}^{ini} and the unstable fracture toughness K_{Ic}^{un} is due to the cohesion toughness K_{Ic}^{c}. The cohesion toughness K_{Ic}^{c} can be regarded as the energy absorbed in the progressively extending fictitious crack zone. Therefore, it can be evaluated using the following simple relationship:

$$K_{\mathrm{Ic}}^{ini}=K_{\mathrm{Ic}}^{un}-K_{\mathrm{Ic}}^{c}, \tag{17}$$

where K_{Ic}^{c} is the cohesion toughness that results from the cohesive force on the fictitious crack zone. For three-point bending beams, it can be evaluated by equation (11) and K_{Ic}^{un} can be done by Equation (15).

If the expression of softening traction-separation law and the cohesive force distribution $\sigma(x)$ are carefully chosen to fit completely the properties of the fictitious crack zone, it can be expected that the value of K_{Ic}^{ini} that is determined by inserting the corresponding initial cracking load P_{ini} and the initial crack length a_0 into (15) could exactly be equal to the net stress intensity factor at the effective crack tip at the critical situation. However, to facilitate the analytical solution, certain simplifications have to be used. Hence, some disparity in practical calculation might be possible.

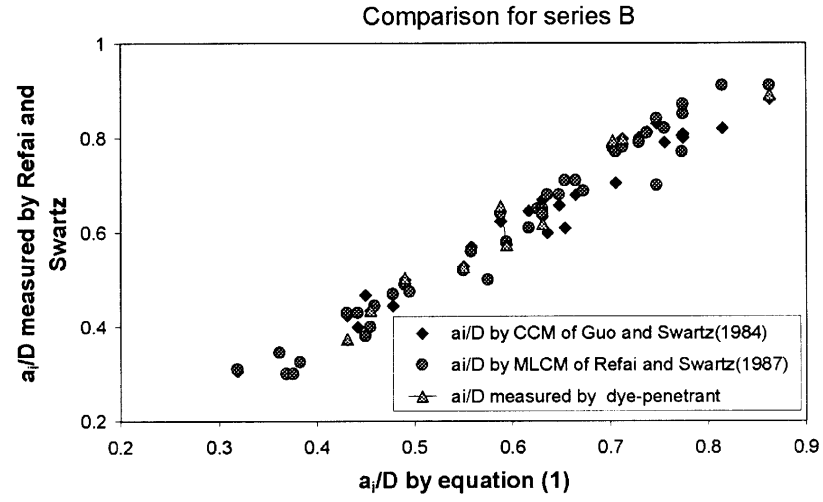


Figure 11. The comparison between the initial crack lengths evaluated by equation (1) based on the linear asymptotic superposition assumption and those measured as well as evaluated in (Refai and Swartz, 1987b): (a) for series B beams; and (b) for series C beams.

In addition, one needs to know CTOD_c to use the σ-w relation (6) to give a determined cohesive force distribution (5). Once, CMOD_c is measured in tests, CTOD_c can be evaluated by the following expression (Jenq and Shah, 1985b):

$$\mathrm{COD}(x) = \mathrm{CMOD}_c \left\{ \left(1 - \frac{x}{a}\right)^2 + \left(1.081 - 1.149\frac{a}{D}\right)\left[\frac{x}{a} - \left(\frac{x}{a}\right)^2\right] \right\}^{1/2}. \tag{18}$$

For obtaining CTOD_c, one must replace x and a in (18) by a_0 and a_c respectively. Equation (18) is suitable for the three-point bending beam for $\mathrm{S} = 4\mathrm{D}$.

Now, if one carries out a fracture test on a single size three-point bending beam to measure a monotonous loading P-CMOD curve (its descending branch is not necessary) the double-K fracture parameter K_{Ic}^{ini} and K_{Ic}^{un}, as well as CTOD_c can be analytically evaluated based on the approaches above. The detailed determination procedure contains the following steps:

(1) Calculate Young's modulus E using (3) according to the initial compliance c_i measured from the linear segment of the P-CMOD curve. If only $P_{\max}$ and CMOD_c were measured, using the experimental results of Karihaloo and Nallathambi (1991) Young's modulus measured from compressive cylinder tests can be used, instead of that received from P-CMOD curve;
(2) Insert the measured maximum load $P_{\max}$, CMOD_c and Young's modulus E into (1) to calculate the critical crack length a_c;
(3) Evaluate CTOD_c by (18) using the measured CMOD_c and the calculated a_c. Then insert the CTOD_c into (6) or (8), and the value of σ_s in (5) can be gained. So, the cohesive force distribution $\sigma(x)$ on the fictitious crack zone is completely determined.
(4) Carry out a numerical scheme to get the integral value of K_{Ic}^{c} for integration (11);
(5) Submit the measured maximum load $P_{\max}$ and the evaluated a_c into (15), and the unstable fracture toughness K_{Ic}^{un} can be obtained;
(6) Finally insert the values of K_{Ic}^{un} and K_{Ic}^{c} into (17), and the initiation toughness K_{Ic}^{ini} can be got too.

6. Experimental verification

According to the determination method of the double-K fracture parameters, one needs to measure the initial compliance c_i, maximum load $P_{\max}$ and the critical crack mouth opening displacement CMOD_c in tests on three-point bending notched beams. Experiments on three-point bending beams had been carried out by various researchers (Jenq and Shah, 1985a, 1985b; Nallathambi and Karihaloo, 1986, 1989, 1990; Swartz and Go, 1984; Swartz and Refai, 1987a; Refai and Swartz, 1987b; Karihaloo and Nallathambi, 1991; Hilsdorf and Brameshuber, 1984; Bascoul, et al. 1987; Xu and Zhao, 1989, 1991). However, the published literature (Jenq and Shah, 1985a, 1985b; Nallathambi and Karihaloo 1986; Karihaloo and Nallathambi 1989, 1990; Swartz and Go, 1984; Swartz and Refai, 1987a; Karihaloo and Nallathambi 1991; Hilsdorf and Brameshuber, 1984; Bascoul, et al. 1987; Xu and Zhao, 1989, 1991) did not supply the complete information of P-CMOD curves for all tested beams. However, in the report of Refai and Swartz (1987b), complete P-CMOD curves measured from all tested beams were enclosed. So, experimental verification for the determination methods is provided based on the tests (Refai and Swartz, 1987b).

The results measured from the experiments of two series of three-point bending beams (Refai and Swartz, 1987b) are utilized to evaluate the double-K fracture parameters K_{Ic}^{ini} and K_{Ic}^{un}. The first series of the beams is denoted with series B, of which, the dimensions are $762 \times 203 \times 76$ mm (span $\times$ depth $\times$ thickness). And the second series is denoted with series C with dimensions of $1143 \times 305 \times 76$ mm (span $\times$ depth $\times$ thickness). All two series of the beams were made with the same mix proportions of 1:2.468:3.585:0.50 (cement:sand:coarse aggregate:water by wt.). The maximum size of the coarse aggregate is 19 mm. The normal cylinder compressive strength of 53.1 MPa and a modulus of elasticity of 38.4 GPa for series B beams, 54.4 MPa and 39.3 GPa for series C correspondingly.

Table 2. Comparison between the initial crack lengths evaluated and measured for series B. ($S \times D \times B = 762 \times 203 \times 76$ mm, $H_0 = 3.2$ mm).

Nos. of specs.	Initial compliance $c_i \times 10^{-6}$ (mm/N)	a_i/D by Equation (1)	a_i/D by CCM of Guo and Swartz (1987b)	(4)/(3)	a_i/D by MLCM of Refai and Swartz (1987b)	(6)/(3)	a_i/D measured by dye-penetrant (1987b)	(8)/(3)
(1)	(2)	(3)	(4)	(5)	(6)	(7)	(8)	(9)
B4	4.489	0.319	0.305	0.956	0.31	0.972		
B17	5.612	0.362			0.345	0.953		
B33	5.836	0.369			0.3	0.813		
B15	6.061	0.376			0.3	0.798		
B1	6.289	0.383			0.325	0.849		
B36	8.081	0.431	0.424	0.984	0.43	0.998	0.375	0.87
B3	8.575	0.442	0.4	0.905	0.43	0.973		
B31	8.979	0.45	0.468	1.04	0.38	0.844		
B37	9.203	0.455	0.435	0.956	0.4	0.879	0.436	0.958
B20	9.428	0.459			0.445	0.969		
B18	10.46	0.478	0.445	0.931	0.47	0.983		
B40	11.134	0.49	0.5	1.02	0.49	1	0.504	1.029
B19	11.493	0.495			0.475	0.96		
B45	15.713	0.55	0.528	0.96	0.52	0.945	0.528	0.96
B5	16.498	0.558	0.57	1.022	0.56	1.004		
B34	18.249	0.575			0.5	0.87		
B39	19.758	0.588	0.624	1.061	0.64	1.088	0.656	1.116
B44	20.479	0.594	0.575	0.968	0.58	0.976	0.575	0.968
B25	23.799	0.617	0.646	1.047	0.61	0.989		
B21	25.146	0.626	0.65	1.038	0.65	1.038		
B22	26.044	0.631	0.67	1.062	0.65	1.03		
B38	26.044	0.631	0.634	1.005	0.64	1.014	0.619	0.981
B8	26.942	0.636	0.6	0.943	0.68	1.069		
B7	29.189	0.648	0.658	1.015	0.68	1.049		
B10	30.534	0.654	0.61	0.933	0.71	1.086		
B24	32.869	0.665	0.68	1.023	0.71	1.068		
B32	35.025	0.673			0.688	1.022		
B42	43.808	0.703	0.775	1.102	0.78	1.11	0.794	1.129
B9	44.903	0.706	0.705	0.999	0.77	1.091		
B41	47.459	0.713	0.798	1.119	0.78	1.094	0.798	1.119
B28	54.76	0.73	0.8	1.096	0.79	1.082		

Table 2. Contd. Comparison between the initial crack lengths evaluated and measured for series B. ($S \times D \times B = 762 \times 203 \times 76$ mm, $H_0 = 3.2$ mm).

Nos. of specs.	Initial compliance $c_i \times 10^{-6}$ (mm/N)	a_i/D by Equation (1)	a_i/D by CCM of Guo and Swartz (1987b)	(4)/(3)	a_i/D by MLCM of Refai and Swartz (1987b)	(6)/(3)	a_i/D measured by dye-penetrant (1987b)	(8)/(3)
(1)	(2)	(3)	(4)	(5)	(6)	(7)	(8)	(9)
B30	58.411	0.738	0.812	1.1	0.81	1.098		
B29	63.887	0.748	0.83	1.11	0.84	1.123		
B35	63.887	0.748			0.7	0.936		
B27	68.998	0.756	0.79	1.045	0.82	1.085		
B26	82.14	0.774	0.805	1.04	0.77	0.995		
B11	82.623	0.775	0.8	1.032	0.85	1.097		
B12	82.623	0.775	0.808	1.043	0.87	1.123		
B13	126.63	0.815	0.82	1.006	0.91	1.117		
B43	242.77	0.863	0.882	1.022	0.91	1.054	0.891	1.032
Mean				1.019		1.006		1.016
S.D.				0.056		0.089		0.085
C.V.				0.055		0.088		0.084

It must be noted that before a beam of series B and C (Refai and Swartz, 1987b) was tested to failure to measure a complete P-CMOD curve and P-δ curve, a crack was initially precracked to a designed size by using strain control. The initial precracked crack lengths of ten specimens in the series B and fourteen specimens in the series C were directly measured using a dye-penetrant technique. Then the authors carried out a satisfactory regression analysis to gain the expressions of the compliance calibration curve and the maximum load calibration curve. As the results, the lengths of initial precracked cracks a_i of other specimens were evaluated. These data of the lengths of initial precracked cracks gained by both direct measuring and evaluating approaches in (Refai and Swartz, 1987b) can be taken as a direct prove for the method to determine the effective crack length using the linear asymptotic superposition assumption. Therefore, each initial compliance c_i for each beam was carefully measured according to P-CMOD curves of all two series beams presented in the report (Refai and Swartz, 1987b). Using the measured values of the initial compliance c_i, the lengths of the initial precracked cracks a_i can be analytically calculated according to (1).

Therefore, using the initial compliance c_i measured from the P-CMOD curves presented in (Refai and Swartz, 1987b) the related lengths of the initial precracked cracks to the depth of beams using the linear asymptotic superposition assumption are evaluated by (1). The results are given in Table 2 and Table 3 for series B and C separately. Of course, due to higher order in (1) a trial and error method has to be used in the computation. The corresponding values of a_i/D obtained by the dye-penetrant technique and regression expressions in the report (Refai and Swartz, 1987b) are illustrated in Table 2 and Table 3 too. It can be found that the values of a_i/D evaluated by equation (1) are in very good agreement with those gained by the approaches in (Refai and Swartz, 1987b). The relative errors of a_i/D values evaluated by

Table 3. Comparison between the initial crack lengths evaluated and measured for series C. ($S \times D \times B = 1143 \times 305 \times 76$ mm, $H_0 = 3.2$ mm).

Nos. of specs.	Initial compliance $c_i \times 10^{-6}$ (mm/N)	a_i/D by Equation (1)	a_i/D by CCM of Guo and Swartz (1987b)	(4)/(3)	a_i/D by MLCM of Refai and Swartz (1987b)	(6)/(3)	a_i/D measured by dye-penetrant (1987b)	(8)/(3)
(1)	(2)	(3)	(4)	(5)	(6)	(7)	(8)	(9)
C23	5.963	0.379	0.404	1.066	0.42	1.108	0.375	0.989
C22	6.017	0.381	0.417	1.094	0.33	0.866	0.381	1.0
C1	6.737	0.403	0.494	1.226	0.39	0.968		
C24	7.634	0.426	0.425	0.998	0.42	0.986	0.433	1.016
C2	8.081	0.437	0.521	1.192	0.42	0.961		
C3	8.216	0.44	0.5	1.136	0.43	0.977		
C15	8.797	0.453	0.569	1.256	0.5	1.104		
C21	9.428	0.465	0.435	0.935	0.43	0.925	0.418	0.899
C4	10.101	0.478	0.528	1.105	0.45	0.941		
C20	11.672	0.504	0.552	1.095	0.51	1.012	0.472	0.937
C16	11.862	0.507	0.577	1.138	0.48	0.947		
C6	12.391	0.515	0.552	1.072	0.52	1.01		
C26	13.468	0.529	0.538	1.017	0.54	1.021	0.568	1.074
C5	14.815	0.546	0.569	1.042	0.52	0.952		
C19	15.056	0.549	0.567	1.033	0.53	0.965	0.52	0.947
C17	15.713	0.556	0.585	1.052	0.54	0.971	0.56	1.007
C7	20.202	0.597	0.631	1.057	0.6	1.005		
C30	22.082	0.611	0.612	1.002	0.63	1.031	0.647	1.059
C29	22.222	0.612	0.623	1.018	0.64	1.046	0.669	1.093
C27	22.761	0.616	0.617	1.002	0.65	1.055	0.652	1.058
C8	25.14	0.631	0.667	1.057	0.52	0.824		
C9	26.308	0.638	0.704	1.103	0.68	1.066		
C28	26.487	0.639	0.643	1.006	0.67	1.049	0.638	0.998
C10	28.286	0.648	0.689	1.063	0.68	1.049		
C11	60.236	0.745	0.705	0.946	0.76	1.02		
C12	62.974	0.75	0.817	1.089	0.8	1.067		
C13	77.577	0.772	0.867	1.123	0.82	1.062		
C31	79.403	0.774	0.792	1.023	0.79	1.021	0.761	0.983
C25	127.77	0.818	0.867	1.06	0.84	1.027	0.884	1.081
C14	131.42	0.82	0.867	1.057	0.82	1.0		
Mean				1.069		1.001		1.01
S.D.				0.074		0.065		0.058
C.V.				0.069		0.064		0.057

中国科技论文在线 www.paper.edu.cn

Table 4. The results of double-K fracture parameters K_{Ic}^{ini} and K_{Ic}^{un} determined for series B. ($S \times D \times B = 762 \times 203 \times 76$ mm, $H_0 = 3.2$ mm, $f_c' = 53.1$ MPa, $E = 38.4$ GPa)

Nos. of specs.	$c_i \times 10^{-6}$ (mm/N)	a_i/D	P_{max} (N)	CMOD$_c$ (mm)	CTOD$_c$ (mm)	a_c/D	K_{Ic}^{c} (MPa m$^{1/2}$)	K_{Ic}^{ini} (MPa m$^{1/2}$)	K_{Ic}^{un} (MPa m$^{1/2}$)
B1	6.289	0.383	5523	45.9	12.67	0.436	0.566	0.795	1.361
B3	8.575	0.442	4365	51.1	12.98	0.499	0.599	0.709	1.308
B4	4.489	0.319	5612	43.4	17.89	0.422	0.822	0.507	1.33
B5	16.498	0.558	3207	89.5	21.07	0.641	0.75	0.883	1.634
B7	29.189	0.648	2249	89.4	12.79	0.69	0.536	0.922	1.457
B8	26.942	0.636	2227	80	11.55	0.677	0.525	0.828	1.354
B9	44.903	0.706	1537	92.8	10.46	0.742	0.503	0.843	1.346
B10	30.534	0.654	2004	77.4	9.59	0.687	0.468	0.818	1.286
B11	82.623	0.775	980	116.6	10.36	0.809	0.519	0.902	1.422
B12	82.623	0.775	891	120.6	12.19	0.82	0.625	0.905	1.43
B13	126.63	0.815	579	130.2	10.97	0.858	0.657	0.757	1.415
B15	6.061	0.376	5033	43.1	13.23	0.442	0.641	0.622	1.264
B16	4.265	0.309	5790	44	18.89	0.419	0.849	0.51	1.358
B17	5.612	0.362	5166	53.3	21.01	0.476	0.872	0.563	1.436
B18	10.46	0.478	4053	65.5	17.54	0.555	0.702	0.766	1.468
B19	11.493	0.495	3919	58	11.83	0.54	0.527	0.822	1.349
B20	9.428	0.459	4187	61.4	17.3	0.538	0.714	0.716	1.43
B21	25.146	0.626	2450	86.8	14	0.675	0.576	0.894	1.47
B22	26.044	0.631	2450	107.4	20.27	0.703	0.714	0.971	1.686
B24	32.869	0.665	1982	86.6	11.26	0.703	0.51	0.865	1.375
B25	23.799	0.617	2784	94	15.71	0.668	0.577	1.031	1.608
B26	82.14	0.774	1559	329.9	43.05	0.854	0.856	2.363	3.219
B27	69.998	0.756	1203	130.5	14.05	0.801	0.594	1.003	1.597
B28	54.76	0.73	1403	141.5	19.5	0.794	0727	1.019	1.746
B29	63.887	0.748	1069	171.1	25.32	0.833	0.953	0.932	1.885
B30	58.411	0.738	1292	145.5	19.93	0.804	0.758	0.99	1.748
B31	8.979	0.45	4855	82.8	27.49	0.564	0.861	0.945	1.806
B32	35.025	0.673	2138	101.5	13.16	0.713	0.515	1.044	1.559
B33	5.836	0.369	4832	64	27.49	0.521	1.047	0.502	1.549
B34	18.249	0.575	2494	90.3	22.46	0.678	0.895	0.62	1.515
B35	63.887	0.748	891	107.8	13.92	0.811	0.777	0.546	1.323
B36	8.081	0.431	4409	62.8	20.81	0.533	0.827	0.652	1.479
B37	9.203	0.455	4676	73.8	22.73	0.551	0.784	0.88	1.664
B38	26.044	0.631	2539	100	17.17	0.689	0.627	1	1.627
B39	19.758	0.588	2539	87.8	19.48	0.672	0.782	0.716	1.497
B40	11.134	0.49	3830	80.8	24.44	0.599	0.868	0.762	1.63
B41	47.459	0.713	1514	158.5	25.99	0.798	0.87	1.05	1.919
B42	43.808	0.703	1515	184.6	34.54	0.811	1.056	1.074	2.13
B43	242.77	0.863	579	182	7.23	0.878	0.353	1.441	1.794
B44	20.479	0.594	3073	95.5	18.49	0.657	0.641	1.035	1.677
B45	15.713	0.55	3563	80	16.43	0.608	0.606	0.974	1.581
Mean					17.355		0.695	0.843	1.538
S. D.					5.86		0.161	0.191	0.193
C. V.					0.338		0.232	0.227	0.125

中国科技论文在线 www.paper.edu.cn

Table 5. The results of double-K fracture parameters K_{Ic}^{ini} and K_{Ic}^{un} determined for series C. ($S \times D \times B = 1143 \times 305 \times 76$ mm, $H_0 = 3.2$ mm, $f_c' = 54.4$ MPa, $E = 39.3$ GPa)

Nos of specs..	c_i (mm/N)	a_i/D	$P_{\max}$ (N)	CMOD$_c$ (mm)	CTOD$_c$ (mm)	a_c/D	K_{Ic}^{c} (MPa m$^{1/2}$)	K_{Ic}^{ini} (MPa m$^{1/2}$)	K_{Ic}^{un} (MPa m$^{1/2}$)
C1	6.737	0.403	6547	100.4	40.33	0.552	1.229	0.706	1.935
C2	8.081	0.437	6057	106.8	39.16	0.575	1.179	0.773	1.952
C3	8.216	0.44	5879	96.0	33.45	0.562	1.093	0.721	1.814
C4	10.101	0.478	5612	98.8	29.16	0.575	0.949	0.865	1.814
C5	14.815	0.546	4543	100.8	22.07	0.612	0.779	0.932	1.711
C6	12.391	0.515	4543	108.5	31.18	0.623	1.046	0.744	1.791
C7	20.202	0.597	3385	107.0	21.13	0.664	0.814	0.81	1.625
C8	25.14	0.631	3207	120.4	20.43	0.687	0.742	0.984	1.726
C9	26.308	0.638	2450	124.0	25.06	0.725	1.006	0.639	1.645
C10	28.286	0.648	2494	130.9	24.98	0.729	0.956	0.755	1.711
C11	60.236	0.745	1514	185.0	25.19	0.814	0.947	1.022	1.969
C12	62.974	0.75	1269	142.3	17.47	0.807	0.856	0.75	1.606
C13	77.577	0.772	846	168.9	22.32	0.852	1.199	0.557	1.756
C14	131.42	0.82	868	198.2	15.76	0.861	0.739	1.232	1.971
C15	8.797	0.453	4899	99.4	36.02	0.598	1.259	0.481	1.739
C16	11.862	0.507	5077	120.3	35.93	0.622	1.069	0.908	1.977
C17	15.713	0.556	4276	98.4	20.47	0.617	0.756	0.896	1.653
C19	15.056	0.549	4498	101.6	22.12	0.615	0.78	0.934	1.714
C20	11.672	0.504	4676	96.4	26.95	0.6	0.969	0.712	1.681
C21	9.428	0.465	5879	82.8	22.13	0.537	0.8	0.862	1.662
C22	6.017	0.381	7660	68.4	21.95	0.455	0.803	0.849	1.653
C23	5.963	0.379	6013	64.0	23.89	0.488	1.024	0.422	1.446
C24	7.634	0.426	6124	64.4	17.16	0.485	0.729	0.733	1.462
C25	127.77	0.818	668	135.0	10.1	0.853	0.693	0.81	1.503
C26	13.468	0.529	4276	76.0	14.8	0.576	0.661	0.752	1.413
C27	22.761	0.616	2895	87.2	13.3	0.657	0.64	0.727	1.367
C28	26.487	0.639	2628	97.6	15.0	0.686	0.693	0.739	1.432
C29	22.222	0.612	2984	86.0	12.84	0.651	0.617	0.749	1.366
C30	22.082	0.611	3118	92.5	14.65	0.655	0.654	0.794	1.449
C31	79.403	0.774	1203	119.1	8.47	0.796	0.483	0.93	1.413
C32	5.163	0.352	7571	72.2	29.12	0.468	1.032	0.662	1.695
C33	15.238	0.551	3697	99.3	24.59	0.641	0.961	0.629	1.59
C34	45.634	0.712	1514	95.5	10.9	0.75	0.652	0.605	1.257
Mean					22.669		0.873	0.778	1.651
S.D.					8.235		0.196	0.156	0.192
C.V.					0.363		0.225	0.201	0.116

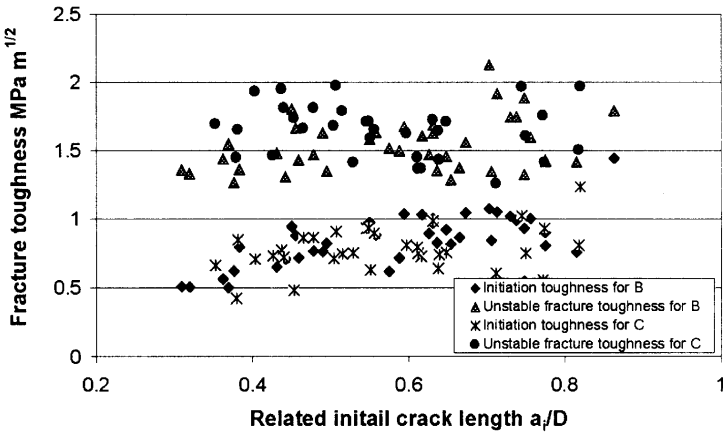


Figure 12. The values of K_{Ic}^{ini} and K_{Ic}^{un} measured for the series B and C beams.

(1) compared to ones by the compliance calibration method (CCM) are listed in the column (5), those compared to ones evaluated by the maximum load calibration method (MLCM) in the column (7) and compared to ones measured by dye-penetrant technique in the column (9) correspondingly. The mean error is less 2 percent compared with those measured by the dye-penetrant technique and is less 1 percent compared with those evaluated by MLCM and less 7 percent compared with those evaluated by CCM respectively for both series B and C beams. The corresponding coefficients of variation are less 8 percent, 9 percent and 7 percent respectively.

The comparison results are illustrated in Figure 11 too. The related initial crack length a_i/D, that are evaluated using the initial compliance measured from P-CMOD curves presented in (Refai and Swartz, 1987b) through (1) based on the linear asymptotic superposition assumption proposed in this paper, is taken as the horizontal axle. As contrary, the values of the related initial crack length gained by the two calibration methods and measured by dye-penetrant technique in (Refai and Swartz, 1987b) are plotted in the vertical axis. It can be seen that the most points fell to the diagonal lines. So, the proposed method to evaluate the crack length based on the linear asymptotic superposition assumption has been verified by the experimental evidence provided by the experiments (Refai and Swartz, 1987b).

So, when Equation (1) is utilized to evaluated the crack lengths of three-point bending beams, one only needs to measure the secant compliance at the maximum load in tests. Both unloading produce used in (Jenq and Shah, 1985a, 1985b) and satisfactory regression used in (Refai and Swartz, 1987b) can be avoided in the evaluation of effective crack length. Now, we begin to use the above-mentioned calculating procedures to determine the double-K fracture parameters K_{Ic}^{ini} and K_{Ic}^{un} using the testing data provided in (Refai and Swartz, 1987b). The calculations has been programmed with Fortran. In our computation for the tests of series B and C beams, we only need to input the data dealing with the modulus of elasticity E, compressive strength f_c, initial compliance c_i and the critical crack mouth opening displacement CMOD_c, as well as geometrical parameters. For convenience, the expression of softening traction-separation law shown in (6) and corresponding $c_1 = 3, c_2 = 7$ and $w_0 = 160$ μm were used. Then, these values of the related length of the initial precracked crack to the depth a_i/D, the related lengths of the critical effective crack to the depth a_c/D and the critical crack tip opening displacement CTOD_c, as well as the cohesion toughness K_{Ic}^{c} were obtained in the

Table 6. The comparison between values of K_{Ic}^{un} evaluated by (17) and measured in tests.

Nos. of specimens	P_{ini} (N)	K_{Ic}^{ini} (MPa m$^{1/2}$) by formula of LEFM using a_0 and p_{ini}	$P_{\max}$ (N)	K_{Ic}^{un} (MPa m$^{1/2}$) by formula of LEFM using a_c and $p_{\max}$	K_{Ic}^{c} (MPa m$^{1/2}$) by formula (11)	$K_{\mathrm{Ic}}^{un} = K_{\mathrm{Ic}}^{ini} + K_{\mathrm{Ic}}^{c}$ (MPa m$^{1/2}$) by (17)	relative errors (7)/(5)
(1)	(2)	(3)	(4)	(5)	(6)	(7)	(8)
C1BL	9224	0.557	13907	1.121	0.555	1.112	0.992
C1BM	5712	0.531	8486	1.048	0.514	1.045	0.997
C1BS	2959	0.505	4200	1.003	0.504	1.009	1.006

computation. Next, the unstable fracture toughness K_{Ic}^{un} is calculated. Finally, initial cracking toughness K_{Ic}^{ini} was evaluated. The all values evaluated were output in an output file. The values of them are presented in Table 4 and Table 5 for series B and C respectively.

The average values of K_{Ic}^{ini} and K_{Ic}^{un} for the series B are 0.843 MPa m$^{1/2}$ and 1.538 MPa m$^{1/2}$ correspondingly. These values for the series C are 0.778 MPa m$^{1/2}$ and 1.651 MPa m$^{1/2}$ correspondingly. The coefficients of variation of the measured values for series B are 0.227 and 0.125 correspondingly. These values for series C are 0.201 and 0.116 correspondingly. In the region of the tested specimen sizes, the evaluated values of K_{Ic}^{un} and K_{Ic}^{ini} are size-independent. It can be also observed that the coefficients of variation of the measured values K_{Ic}^{ini} and K_{Ic}^{un} are in the same range as those for normal strength parameters of concrete like f_t, f_c. For example, the coefficients of variation of the measured values of f_t, f_c for the series B cylinder data are 0.057 and 0.229 correspondingly. When the values of K_{Ic}^{ini} and K_{Ic}^{un} measured from two series of B and C beams with different dimensions are presented in Figure 12, no observable difference for the series B and C beams can be observed.

But, the mean values of CTOD$_c$ measured from the two series beams seems size-dependent. For the series B the mean value of CTOD$_c$ is 17.35 μm and for series C it is 22.67 μm.

Herein, the instances of numerical experiments performed in (Reinhardt and Xu, 1998a; 1998b) that the initial cracking load P_{ini} was carefully distinguished are utilized to check equation (17). The formula (11) is applied to evaluation of the cohesion toughness K_{Ic}^{c} for three-point bending beams. The results are given in Table 6. It can be seen that a satisfactory predication can be gained by formula (11).

In fact, the influence of the shapes of σ-w curves on evaluation of the cohesion toughness K_{Ic}^{c} are not observable. When the instance presented in Table 6 is utilized to evaluate the values of the cohesion toughness K_{Ic}^{c} using the three different formulae (11), (12) and (13) developed from different crack cases based on the three σ-w relationships expressed by the expressions (6), (7) and (14) respectively, the results evaluated are given in Table 7. It can be seen that the differences between the values of cohesion toughness K_{Ic}^{c} evaluated by each one among the formulae (11), (12) and (13) based on the three different σ-w relations are not significant. Therefore, when a purpose of convenience is considered, the simplified bilinear softening σ-w relationship expressed in (7) and (8) based on a modified approach for CEB-FIP Model Code 1990 could be engaged in practical calculation.

It can be seen that for a three-point bending notched beam the integration expression (11) has good accuracy to calculate the cohesion toughness K_{Ic}^{c}. But, if the formulae (12) and (13) are used to do an approximate estimation, some error could be expected for some cases because they are not in conformity with the geometrical conditions.

.

Table 7. The comparison between the results of by different σ-w relations.

Nos. of specimens	The parameters used in different σ-w equations			K_{Ic}^{c} (MPa m$^{1/2}$) by formula (11)			K_{Ic}^{c} (MPa m$^{1/2}$) by formula (12)			K_{Ic}^{c} (MPa m$^{1/2}$) by formula (13)		
	σ-w Equation (6) (c_1, c_2, w_0)	σ-w Equation (7) (β)	σ-w Equation (14) (k, λ)	By σ-w (6)	By σ-w (7)	By σ-w (14)	By σ-w (6)	By σ-w (7)	By σ-w (14)	By σ-w (6)	By σ-w (7)	By σ-w (14)
(1)	(2)	(3)	(4)	(5)	(6)	(7)	(8)	(9)	(10)	(11)	(12)	(13)
C1BL	$c_1 = 3$	0.146	$k = 0.0616$	0.549	0.555	0.570	0.531	0.536	0.547	0.524	0.529	0.540
C1BM	$c_2 = 10$	0.167	$\lambda = 1.01$	0.511	0.514	0.535	0.487	0.489	0.505	0.481	0.483	0.498
C1BS	$w_0 = 110\,\mu$m	0.175		0.503	0.504	0.530	0.459	0.460	0.478	0.451	0.452	0.469

中国科技论文在线 www.paper.edu.cn

However, the experimental evidence shows that the determining method of the double-K fracture parameters K_{Ic}^{ini} and K_{Ic}^{un} for three-point bending beams proposed in this paper only needs to measure the ascending branch of P-CMOD curve of the testing beam even though only the maximum load $P_{\max}$ and CMOD_c. An unloading and reloading procedure during the testing can be avoided. In the practical measurement for them, one only carries out tests on a single size three-point bending beams on a common testing machine without a closed-loop testing system. For most common materials and structures laboratories, this testing method is very practical. In evaluation for the parameters, testing workers do not need any satisfactory regression for evaluating the critical crack length. All parameters can be analytically evaluated. Enough testing data verified that the double-K fracture parameters K_{Ic}^{ini} and K_{Ic}^{un} are size-independent. Therefore, the determining method of the double-K fracture parameters K_{Ic}^{ini} and K_{Ic}^{un} for three-point bending beams proposed has the potentiality to be a standard testing method.

7. Conclusions

A new crack propagation criterion, the so-called double-K criterion, is proposed to describe both cracking initiation and critical unstable fracture situations. The presentation of the double-K fracture criterion for crack propagation in quasi-brittle materials was possible due to the great preparating material including the basic concept, experimental evidence and evaluating methods to determine the corresponding parameters.

In this paper, an attempt is achieved to look for a practical measuring method for the tests on a single size of three-point bending notched beams and to develop the corresponding analytical evaluating methods for determination of the double-K fracture parameters K_{Ic}^{ini} and K_{Ic}^{un} using the testing data measured from the simple testing procedure.

Based on the knowledge that the nonlinear characteristic appeared on P-CMOD curves is mainly associated with crack propagation, a linear asymptotic superposition assumption is proposed. Based on the assumption, all fracture parameters including CTOD_c, K_{Ic}^{ini} and K_{Ic}^{un} used and introduced in the double-K fracture criterion can be analytically determined using the initial compliance c_i and the secant compliance c_s, even only if the secant compliance c_s was measured from the tests on a single size of three-point bending notched beams. The testing procedure is very simple without unloading and reloading procedures. It only needs to apply monotonously a load on a beam until the maximum load is gained and to measure the rising branch of a P-CMOD curve. For achieving such an aim to measure c_i and c_s in tests, a closed-loop testing system is not necessary. For most common materials and structures laboratories, this testing method is very practical.

With regard to the difference between the crack length measured in the interior of the specimen and that observed on the surface, the method proposed is further developed to base on the measurement of average crack length along the whole section of the specimens that includes the crack length both on the surface and in the interior. The results predicted by this method are in very good agreement with the measurement of the average crack length of the whole section of the specimen using the dye-penetrant technique by Swartz and Refai in 1987.

The experimental evidence shows that the measured double-K fracture parameters K_{Ic}^{ini} and K_{Ic}^{un} are size-independent in the region of the tested specimen sizes and can be employed to describe the cracking initiation and critical unstable fracture of concrete structures with cracks. For the critical crack tip opening displacement CTOD_c evaluated seems to be size-

中国科技论文在线 www.paper.edu.cn

dependent in the region of the tests. It needs to be confirmed in future studies. Otherwise, further verification by the tests on three-point-bending notched beams with different depths from 100 mm to 400 mm is specially needed because there may be a condition of minimum depth of specimen for measuring the double-K fracture parameters K_{Ic}^{ini} and K_{Ic}^{un}.

Acknowledgement

The first author (SX) acknowledges that the National Natural Science Foundation of China (NNSFC) has partly supported this work.

References

Bascoul, A., Kharchi, F. and Maso, J.C. (1987). Concerning the measurement of the fracture energy of a macro-concrete according to the crack growth in a *Three Points Bending Test on Notched Beams*. SEM/RILEM International Conference on Fracture of Concrete and Rock (Edited by S.P. Shah and S.E. Swartz), Houston, Texas, 396–408.

Bazant, Z.P. and Kazemi, M.T. (1990). Determination of fracture energy, process zone length and brittleness number from size effect, with application to rock and concrete. *International Journal of Fracture* **44**, 111–131.

CEB-Comite Euro-International du Beton- EB-FIP Model Code 1990, Bulletin D'Information No. 213/214, Lausanne. 1993.

Gopalaratnam, V.S. and Shah, S.P. (1985). Softening response of plain concrete in direct tension. *ACI Journal* 310–323.

Hillerborg, A. (1983). Analysis of one single crack. *Fracture Mechanics of Concrete* (Edited by Wittmann), Elsevier Science Publishers, Amsterdam, 223–249.

Hilsdorf, H.K. and Brameshuber, W. (1984). Size effects in the experimental determination of fracture mechanics parameters. In *Application of Fracture Mechanics to Cementitious Composites*, NATO-Advanced Research Workshop, Illinois.

Jenq, Y.S. and Shah, S.P. (1985a). A fracture toughness criterion for concrete. *Engineering Fracture Mechanical* **21**(5), 1055–1069.

Jenq, Y.S. and Shah, S.P. (1985b). Two parameter fracture model for concrete. *Journal Engineering Mechanical, ASCE* **111**(10), 1227–1241.

Karihaloo, B.L. and Nallathambi, P. (1989). An improved effective crack model for the determination of fracture toughness of concrete. *Cement and Concrete Research* **19**, 603–610.

Karihaloo, B.L. and Nallathambi, P. (1990). Effective crack model for the determination of fracture toughness (K_{IC}^{s}) of concrete. *Engineering Fracture Mechanics* **35**(4/5), 637–645.

Karihaloo, B.L. and Nallathambi, P. (1991). Notched beam test: Mode I fracture toughness. *Fracture Mechanics Test Methods for Concrete*, Report of RILEM Technical Committee 89-FMT (Edited by S.P. Shah and A. Carpinteri), Chapman & Hall, London, 1–86.

Nallathambi, P. and Karihaloo, B.L. (1986). Determination of specimen-size independent fracture toughness of plain concrete. *Magazine of Concrete Research* **38**(135), 67–76.

Refai, T.M.E. and Swartz, S.E. (1987b). *Fracture Behavior of Concrete Beams in Three-Point Bending Considering the Influence of Size Effects*. Report No. 190, Engineering Experiment Station, Kansas State University.

Reinhardt, H.W., Cornelissen, H.A.W. and Hordijk, D.A. (1986). Tensile tests and failure analysis of concrete. *Journal of Structural Engineering* **112**(11), 2462–2477.

Reinhardt, H.W. and Xu Shilang (1998a). Characteristics of crack extension resistance in quasi-brittle materials like concrete. *Engineering Fracture Mechanics*, submitted for publication.

Reinhardt, H.W. and Xu Shilang (1998b). Numerical experiments and characteristics of the New KR-curve for the complete fracture process of three-point beading beams. In *Fracture Mechanics of Concrete Structures*. Proceedings FRAMCOS-3, Aedificatio Publishers, D-79104 Freiburg, Germany, 399–408.

RILEM Technical Committee 89-FMT (1990). Determination of fracture parameters (K_{Ic}^{s} and CTOD_c) of plain concrete using three-point bend tests, proposed RILEM draft recommendations. RILEM, *Materials and Structures* **23**(138), 457–460.

中国科技论文在线 www.paper.edu.cn

Swartz, S.E. and Go. C.G. (1984). Validity of compliance calibration to cracked concrete beams in bending. *Experimental Mechanics* **24**(2), 129–134.

Swartz, S.E. and Refai, T.M.E. (1987). *Influence of Size on Opening Mode Fracture Parameters for Precracked Concrete Beams in Bending. Proceedings of SEM-RILEM International Conference on Fracture of Concrete and Rock* (Edited by S.P. Shah and S.E. Swartz), Houston, Texas, 242–254.

Tada, H., Paris, P.C. and Irwin, G.R. (1985), *The Stress Analysis of Cracks Handbook*. Paris Productions Incorporated, St. Louis, Missouri, USA.

Tang, T., Ouyang C. and Shah, S.P. (1995) *A Simple Method for Determining Material Fracture Parameters from Peak Load.* Report of NSF Center for Science and Technology of Advanced Cement-Based Materials, Northwestern University, Illinois, USA.

Wittmann, F.H. and Hu, X. (1991). Fracture process zone in cementitious materials. *International Journal of Fracture* **51**, 3–18.

Xu Shilang and Reinhardt, H.W. (1997). Determination of double-*K* criterion for crack propagation in quasi-brittle materials: Part I – Experimental investigation of crack propagation. *International Journal of Fracture*, submitted for publication.

Xu Shilang and Zhao Guofan (1989). A study on fracture process zones in concrete by means of laser speckle photography. *Brittle Matrix Composites 2* (Edited by A.M. Brandt and I.H. Marshall), Elsevier Applied Science, London, 333–341.

Xu Shilang and Zhao Guofan (1991). *Researches on the Fracture Mechanics of Concrete* (in Chinese). The Press of Dalian University of Technology, Dalian, China.